Functionalized Poly(ethylene glycol)-Based Bioassay Surface Chemistry That Facilitates Bio-Immobilization and Inhibits Nonspecific Protein, Bacterial, and Mammalian Cell Adhesion

Gregory M. Harbers,[†,‡] Kazunori Emoto,[§] Charles Greef,[§] Steven W. Metzger,[§] Heather N. Woodward,[§] James J. Mascali,[§] David W. Grainger,[†,||] and Michael J. Lochhead*[,§]

Department of Chemistry, Colorado State University, Fort Collins, Colorado 80523-1872, and Accelr8 Technology Corporation, 7000 North Broadway, Suite 3-307, Denver, Colorado 80221

Received February 22, 2007. Revised Manuscript Received June 20, 2007

This paper describes a new bioassay surface chemistry that effectively inhibits nonspecific biomolecular and cell binding interactions, while providing a capacity for specific immobilization of desired biomolecules. Poly(ethylene glycol) (PEG) as the primary component in nonfouling film chemistry is well-established, but the multicomponent formulation described here is unique in that it (1) is applied in a single, reproducible, solution-based coating step; (2) can be applied to diverse substrate materials without the use of special primers; and (3) is readily functionalized to provide specific attachment chemistries. Surface analysis data are presented, detailing surface roughness, polymer film thickness, and film chemistry. Protein nonspecific binding assays demonstrate significant inhibition of serum, fibrinogen, and lysozyme adsorption to coated glass, indium tin oxide, and tissue culture polystyrene dishes. Inhibition of *Staphylococcus aureus* and *Klebsiella pneumoniae* microbial adhesion in a microfluidic flow cell and inhibition of fibroblast cell adhesion from serum-based cell culture are shown. Effective functionalization of the coating is demonstrated by directing fibroblast adhesion to polymer surfaces activated with an RGD peptide. Batch-to-batch reproducibility data are included. The in situ cross-linked PEG-based coating chemistry is unique in its formulation, and its surface properties are attractive for a broad range of in vitro bioassay applications.

Introduction

Inhibition of nonspecific biomolecular and cellular adhesion to solid surfaces is critical to the performance of in vitro bioassays. Protein nonspecific binding (NSB), for example, is long recognized as limiting the sensitivity of solid-phase assays such as immunoassays and microarrays.[1,2] Further, the emergence of analytical tools in which live, phenotypically correct cells are maintained in culture milieu at synthetic surfaces has created new surface chemistry challenges.[3] Improved surface treatments and coating technologies that provide better nonfouling performance in conjunction with specific attachment chemistries are sought for these applications.

The use of poly(ethylene glycol) (PEG) polymers and PEG-like materials as the active component in nonfouling surface chemistries is well-established and the subject of several reviews.[4−7] A variety of surface treatment methods have been reported, including PEG grafting,[6,8−18] adsorptive chemistries,[19−24] self-assembled monolayers (SAMs),[25−27]

* To whom correspondence should be addressed. E-mail: mike.lochhead@comcast.net. Phone: 303-863-8088. Fax: 303-863-1218.

† Colorado State University.

‡ Current address: Affinergy, Inc., 617 Davis Dr., Suite 100, Durham, NC 27713.

§ Accelr8 Technology Corporation.

|| Current address: Department of Pharmaceutics and Pharmaceutical Chemistry, College of Pharmacy, 30 South 2000 East, Room 301, Salt Lake City, UT 84112-5820.

(1) Butler, J. E. *Methods* **2000**, *22*, 4−23.
(2) Kusnezow, W.; Hoheisel, J. D. *J. Mol. Recognit.* **2003**, *16*, 165−176.
(3) Lang, P.; Yeow, K.; Nichols, A.; Scheer, A. *Nat. Rev. Drug Discovery* **2006**, *5*, 343−356.
(4) Harris, J. M., Ed. *Poly(ethylene Glycol) Chemistry: Biotechnical and Biomedical Applications*; Plenum Press: New York, 1992.
(5) Hoffman, A. S. *J. Biomater. Sci., Polym. Ed.* **1999**, *10*, 1011−1014.
(6) Leckband, D.; Sheth, S.; Halperin, A. *J. Biomater. Sci., Polym. Ed.* **1999**, *10*, 1125−1147.
(7) Ostuni, E.; Chapman, R. G.; Holmlin, R. E.; Takayama, S.; Whitesides, G. M. *Langmuir* **2001**, *17*, 5605−5620.
(8) Gombotz, W. R.; Wang, G. H.; Horbett, T. A.; Hoffman, A. S. *J. Biomed. Mater. Res.* **1991**, *25*, 1547−1562.
(9) Mao, G.; Castner, D. G.; Grainger, D. W. *Chem. Mater.* **1997**, *9*, 1741−1750.
(10) Sofia, S. J.; Premnath, V.; Merrill, E. W. *Macromolecules* **1998**, *31*, 5059−5070.
(11) Emoto, K.; Van Alstine, J. M.; Harris, J. M. *Langmuir* **1998**, *14*, 2722−2729.
(12) Lee, S. W.; Laibinis, P. E. *Biomaterials* **1998**, *19*, 1669−1675.
(13) Jo, S.; Park, K. *Biomaterials* **2000**, *21*, 605−616.
(14) Xia, N.; Hu, Y.; Grainger, D. W.; Castner, D. G. *Langmuir* **2002**, *18*, 3255−3262.
(15) Schlapak, R.; Pammer, P.; Armitage, D.; Zhu, R.; Hinterdorfer, P.; Vaupel, M.; Fruhwirth, T.; Howorka, S. *Langmuir* **2006**, *22*, 277−285.
(16) Bearinger, J. P.; Castner, D. G.; Golledge, S. L.; Rezania, A.; Hubchak, S.; Healy, K. E. *Langmuir* **1997**, *13*, 5175−5183.
(17) Dalsin, J. L.; Lin, L.; Tosatti, S.; Voros, J.; Textor, M.; Messersmith, P. B. *Langmuir* **2005**, *21*, 640−646.
(18) Wazawa, T.; Ishizuka-Katsura, Y.; Nishikawa, S.; Iwane, A. H.; Aoyama, S. *Anal. Chem.* **2006**, *78*, 2549−2556.
(19) Lee, J. H.; Kopecek, J.; Andrade, J. D. *J. Biomed. Mater. Res.* **1989**, *23*, 351−368.
(20) Malmsten, M.; Van Alstine, J. M. *J. Colloid Interface Sci.* **1996**, *177*, 502−512.
(21) Li, J. T.; Carlsson, J.; Lin, J. N.; Caldwell, K. D. *Bioconjugate Chem.* **1996**, *7*, 592−599.

10.1021/cm070509u CCC: $37.00
Published on Web 08/09/2007

and plasma treatments.[28] Outstanding protein and cellular NSB inhibition has been demonstrated in several of these systems.

Despite significant progress, however, many of these surface chemistries suffer from one or more limitations that hinder widespread application. For example, grafting and SAM technologies are typically compatible only with specific, well-defined substrates. Passively adsorbed coating chemistries typically require a charged or hydrophobic surface and can desorb under stringent wash conditions. Many coating methods require multiple, difficult-to-control processing steps to achieve a high quality final film. Robust, readily functionalized PEG-based thin films applicable to a variety of substrates and amenable to scalable manufacturing are not widely known.

The multicomponent, cross-linked polymer surface chemistry described here was designed to address several of these limitations. The single-step coating formulation which can be applied with conventional industrial processing techniques was developed specifically for in vitro bioassay applications and combines covalent surface attachment and cross-linking chemistries within the coating matrix. Significant inhibition of protein, microbial, and mammalian cell adsorption and adhesion on a variety of relevant substrate materials is demonstrated, while selective functionalization of the coating is shown using specific coupling of an RGD peptide that enables cell attachment in a standard cell culture format. Batch-to-batch specific and NSB reproducibility data are also presented.

Experimental Section

Materials. Substrates consisted of borosilicate glass microscope slides (Schott Glass, D263, 75.6 × 25.0 × 1.0 mm), tissue culture polystyrene (TCPS) Petri dishes (BD Falcon), indium tin oxide (ITO) coated glass slides (Delta Technologies, 75 × 25 × 1.1 mm), and SiO_2/Si wafers (Montco Silicon, 125 mm diameter × 0.5 mm thick). Homobifunctional PEG (molecular weight, MW, 3400), with *N*-oxy-succinimide termini on each end of the PEG molecule, was from NOF, Japan. Here we use the common name NHS-PEG-NHS for this molecule, where NHS is the *N*-hydroxy-succinimide leaving group. Additional coating reagents included organosilanes (3-trimethoxysilylpropyl)diethylenetriamine ("aminosilane") and 6-azidosulfonylhexyltriethoxy silane ("azidosilane"; Gelest, Inc.), polyoxyethylene sorbitan tetraoleate (PST), methoxyethylamine (MEA), and solvents dimethylsulfoxide (DMSO) and *N*,*N*-dimethylacetamide (DMAc; reagent grade, used as received, all from Sigma-Aldrich). Goat serum, human fibrinogen (80% clottable), and hen egg white lysozyme were from Sigma-Aldrich. Horseradish peroxidase (HRP)-conjugated goat anti-human fibrinogen and rabbit anti-lysozyme IgG's were from Abcam, Inc. Goat anti-rabbit IgG and rabbit anti-goat IgG, each labeled with the fluorescent dye Alexa555, were from Molecular Probes, Inc., as was the NHS-Alexa555 used for protein labeling. GRGDS was from American Peptide Company, Inc. Buffer salts, bovine serum albumin (BSA, Fraction V), and other laboratory reagents were obtained from Sigma-Aldrich. The acronym PBS designates phosphate buffered saline (0.1 M sodium phosphate, 0.15 M sodium chloride, pH 7.2). PBST is PBS that contains 0.05% Tween 20. Custom 40mer oligonucleotide probes were from Integrated DNA Technologies (IDT, Coralville, IA). Unmodified and amine-modified probes had identical sequences. Complementary 40mer target sequences with and without terminal Alexa555 labels were also from IDT.

Surface Chemistry and Coating Process. *Substrate Cleaning*. Glass and ITO/glass slides were sonicated at 60 °C in alkaline detergent, extensively water rinsed, racked, dried by centrifugation, and stored in a cleanroom drybox until coating (within 24 h of cleaning). SiO_2/Si wafers were cleaned using a Harrick Plasma cleaner (5 min with argon plasma). TCPS dishes were coated as received. Importantly, all clean substrates were used as-is; no silane treatments or other bonding promoters were used.

Coating Formulation. The coating formulation comprises a single mixture of three components described here as (1) the active component, (2) matrix-forming component, and (3) cross-linking component, all mixed in a carrier solvent.[29] The coating components and process are illustrated schematically in Figure 1. The active component is a heterobifunctional PEG molecule (A-PEG-B) with one end group (A) that serves as the functional group in the final coating. The other PEG end group (B), the reactive group, provides covalent attachment within the coating matrix and to certain substrates. PEGs in the molecular weight range of 2000−5000 have been successfully used. In the formulation described here, the active component was a NHS-PEG-aminosilane construct formed by reacting NHS-PEG-NHS (MW ∼ 3400) with (3-trimethoxysilylpropyl)diethylenetriamine (aminosilane) at a 2:1 molar ratio. The A-PEG-B hetero-construct is the desired reaction product. Incomplete reactions and competing reactions likely produce a mixture of reaction products that include A-PEG-B, B-PEG-B, and A-PEG-A. Optimization of reactant concentrations, reaction times, and temperatures is discussed in more detail below.

The matrix-forming component was a non-ionic surfactant containing ethylene oxide repeat units. Polyoxyethylene sorbitan oleates such as the Tween family of surfactants have been successfully used. Here, PST served as the matrix-forming component.

Azidosilane was used as a molecular cross-linker.[30] Upon thermal activation, the azide converts to a reactive nitrene that rapidly and nonspecifically inserts into aliphatic or aromatic bonds within the coating matrix and into organic surfaces such as polystyrene.[31] Additionally, the silane chemistry reacts both with oxide solid surfaces and with the aminosilane component in the mixture.

Conceptually, the coating formulation is designed to provide multiple reaction pathways for converting the soluble three-component mixture to a stable, resilient functional coating through several possible cross-linking, adhesion, and covalent attachment mechanisms upon curing. In contrast to previous PEG brush

(22) Kenausis, G. L.; Voeroes, J.; Elbert, D. L.; Huang, N.; Hofer, R.; Ruiz-Taylor, L.; Textor, M.; Hubbell, J. A.; Spencer, N. D. *J. Phys. Chem. B* **2000**, *104*, 3298−3309.
(23) Ruiz-Taylor, L. A.; Martin, T. L.; Zaugg, F. G.; Witte, K.; Indermuhle, P.; Nock, S.; Wagner, P. *Proc. Natl. Acad. Sci. U.S.A.* **2001**, *98*, 852−857.
(24) Huang, N.-P.; Michel, R.; Voros, J.; Textor, M.; Hofer, R.; Rossi, A.; Elbert, D. L.; Hubbell, J. A.; Spencer, N. D. *Langmuir* **2001**, *17*, 489−498.
(25) Prime, K. L.; Whitesides, G. M. *J. Am. Chem. Soc.* **1993**, *115*, 10714−10721.
(26) Mrksich, M.; Whitesides, G. M. *ACS Symp. Ser.* **1997**, *680*, 361−373.
(27) Ostuni, E.; Chapman, R. G.; Liang, M. N.; Meluleni, G.; Pier, G.; Ingber, D. E.; Whitesides, G. M. *Langmuir* **2001**, *17*, 6336−6343.
(28) Johnston, E. E.; Bryers, J. D.; Ratner, B. D. *Langmuir* **2005**, *21*, 870−881.
(29) Mao, G.; Metzger, S.; Lochhead, M. J. U.S. Patents 6,844,028 and 7,067,194.
(30) Gonzalez, L.; Rodriguez, A.; De Benito, J. L.; Marcos-Fernandez, A. *J. Appl. Polym. Sci.* **1997**, *63*, 1353−1359.
(31) Scriven, E. F. V., Ed. *Azides and Nitrenes*; Academic Press: New York, 1984.

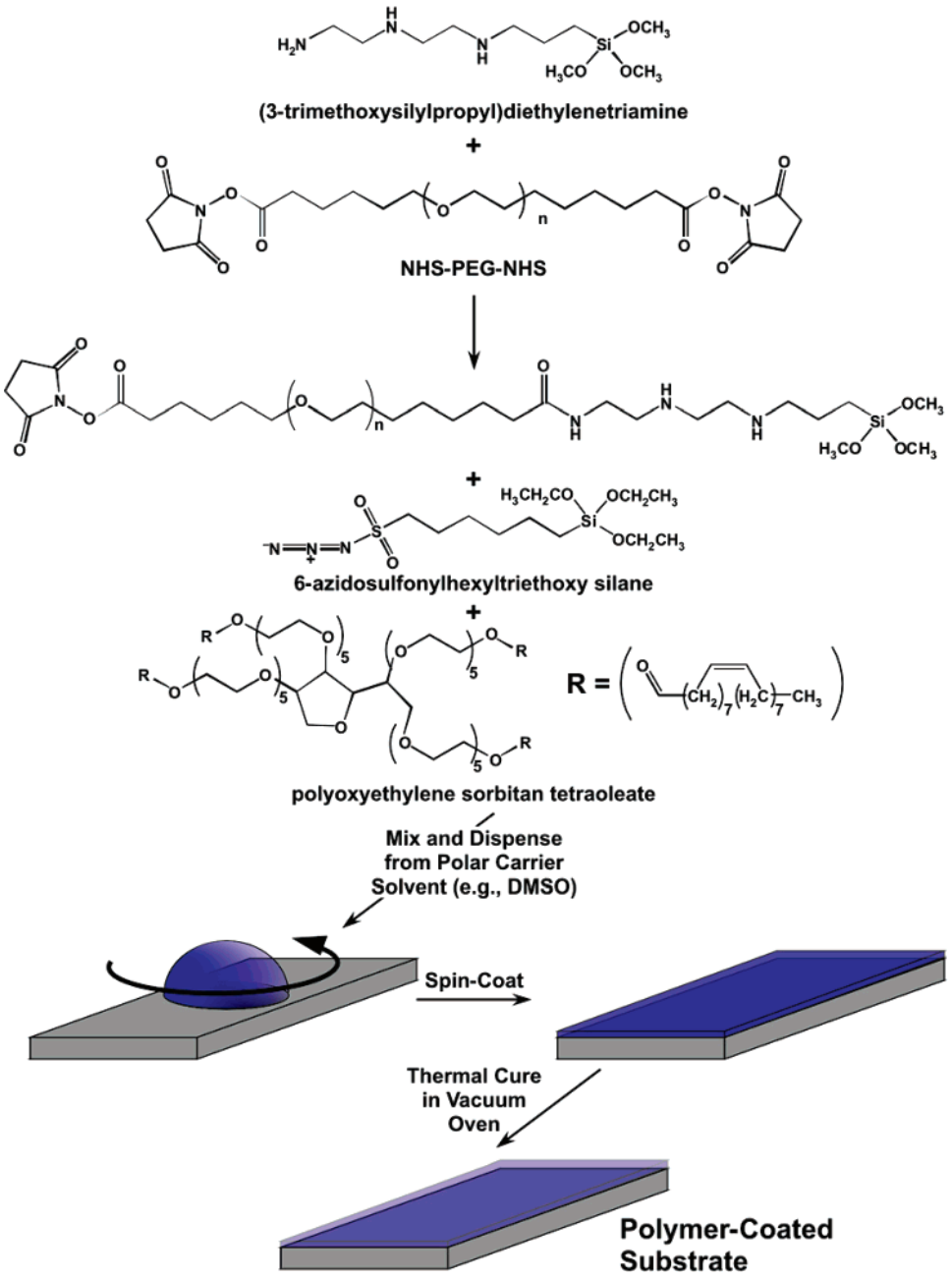

Figure 1. Polymer coating components and process schematic.

technologies that typically rely on end point attachment of polymer chains to the surface or adsorptive chemistries that rely on relatively weak interactions, the intent here is to provide multiple attachment and covalent cross-linking modalities within a single formulation. The amphiphilic matrix forming component is needed to improve the ability to process the coating formulation because removal of this component results in final films that are highly phase-separated and of exceptionally low quality. It has previously been demonstrated that all components are necessary for the formation of the final film.[29]

When engineering the coating formulation, relative reagent concentrations were optimized through extensive functional testing of the final film (contact angle, NHS activity, protein NSB, etc.), rather than analytical characterization of all intermediate reaction products which, although scientifically interesting, was deemed unnecessary because the end goal was to develop a single formulation that was easily applied and resulted in a robust, amine-reactive, low NSB film useful for in vitro diagnostics. For example, the NHS-PEG to aminosilane ratio was optimized to provide reproducible film uniformity while maximizing NHS activity in the final film. The azidosilane cross-linker concentration was optimized to yield a reproducible film surface energy as determined by water contact angle. Removing the azidosilane altogether yielded films with highly variable surface energy that were less stable under stringent wash conditions. Additionally, the azide groups also provide the means for covalent attachment to plastic substrates. Thus, while the formulation may appear to be complex, the reagents, coating process, and curing conditions have been optimized to render a final coating that is relatively insensitive to incompletely characterized intermediate reactions.

The formulation is described in detail here. NHS-PEG-NHS (MW $\sim$ 3400) was mixed with aminosilane at a 2:1 molar ratio in DMAc in a polypropylene conical tube. The reactant concentrations were 19.88 mM NHS-PEG-NHS and 9.89 mM aminosilane, respectively. These were allowed to react at ambient temperature (21−23 °C) with stirring for 2 h. In a separate conical tube, a mixture in DMSO was prepared containing 8.26 mM 6-azidosulfonylhexyltriethoxy silane and 2.17 mM PST. After the 2 h reaction, the DMAc-based

and DMSO-based components were mixed in a 1:5.59 volume ratio with gentle stirring, and additional DMSO was added, yielding final formulation concentrations of 2.52 mM NHS-PEG-NHS, 1.25 mM aminosilane, 5.84 mM azidosilane, and 1.53 mM PST.

This formulation is stable at ambient temperature (21−23 °C) for several days. When stored longer, formulation viscosity increases, likely resulting from silane hydrolysis and condensation. This oligomerization of the coating components results in increased final film thickness. To ensure consistent thickness, all coatings described in this paper were deposited within 48 h of formulation.

Spin Coating, Cure, and Rinse. Solution spin coating used conventional bench top spinners (Laurell Technologies) at 3500 rpm under ambient ventilated conditions unless indicated otherwise. After spinning, the coating was thermally cured at 0.1 mmHg pressure to drive the cross-linking reaction within the film and to remove solvent. Coatings on inorganic substrates were cured for 75 min at 100 °C. For the TCPS, the curing temperature was reduced to 70 °C to avoid substrate softening. After cure, all surfaces were rinsed briefly with ultrapure water to remove any loosely bound material and immediately dried in ambient air in a centrifuge using slide racks in a microplate swing holder. Coated substrates were stored dry in sealed moisture barrier bags with desiccant.

Surface Deactivation. The coating chemistry is designed to provide an NHS-activated polymer coating after cure. Prior to protein NSB and bacterial adhesion assays, reactive NHS groups were quenched by submerging slides in 50 mM MEA in 50 mM borate buffer (pH 9.0) for 1 h at room temperature. The MEA amine terminus reacts with the NHS end groups to create amide-linked ethyl methoxy groups terminating linear PEG chains. For the mammalian cell adhesion assays, NHS groups were hydrolyzed in buffer, resulting in carboxylate-terminated linear PEG chains.

Safety Consideration. All chemical formulation steps and spin operations were performed in certified chemical fume hoods by trained personnel wearing proper personal protective equipment.

Surface Analysis. *Atomic Force Microscopy (AFM)*. AFM measurements were performed on a Digital Instruments NanoScope IIIa. Silicon tips (Nanosensors; resonant frequency of 75−90 Hz; force constant of 2.5−4.4 N/m) were used in tapping mode with a scan rate of 1.00 Hz. Samples were measured both dry (∼40% relative humidity) and under water.

Spectroscopic Ellipsometry. Spectroscopic ellipsometry was used to determine dry polymer film thickness on silicon substrates. All data were collected at room temperature (∼22 °C) and relative humidity (∼40%) using a Woollam VASE VB-250 system equipped with a HS-190 monochromator and controlled by Wvase32 software (Woollam, version 3.398c). For each substrate, data were collected at three incident angles (65°, 70°, and 75°) from 300 to 1100 nm. Experimental Cauchy fits to the spectroscopic data were performed using the Wvase32 software.

X-ray Photoelectron Spectroscopy (XPS). XPS surface analyses were performed as recently described[32] on a Physical Electronics PE5800 ESCA/AES system equipped with a 7 mm monochromatic Al Kα X-ray source (1486.6 eV) and hemispherical analyzer at a 35° photoelectron takeoff angle, defined as the angle between the surface plane and the axis of the analyzer lens. At this angle, sampling depth averages ∼5 nm.

Aqueous Contact Angle (Wetting). All contact angles were measured at ambient conditions (∼22 °C; 30−40% relative humidity) using ultrapure water (ASTM type I water, 18.2 MΩ·cm). Static water contact angle measurements were performed using a custom-built video droplet analysis instrument. Dynamic water contact angles (advancing and receding) were measured using a Krüss drop shape analysis system DSA-10 fitted with a NE43 needle (Krüss USA, Matthews, NC).

Biological Assay Methods. *Protein NSB*. Goat serum was selected as a model system because it mimics a critical assay fluid for in vitro diagnostic and other bioassay formats. Fibrinogen was used because it is a large (340 kD) glycoprotein central to blood clotting and is widely used as a model surface-active protein in NSB assays.[33] Lysozyme (14 kD) was selected because of its unique basic protein character (pI 10.7); lysozyme carries a positive charge at or near neutral pH[34] and has also been widely used as a model NSB protein.[27,35]

Details of the protein NSB immunoassays, including incubation methods, times, and temperatures, are provided in the Supporting Information. Briefly, goat serum was labeled with the fluorescent dye NHS-Alexa555 (Molecular Probes) using vendor protocols, and total protein concentration was determined by BCA assay (Pierce Biotechnology, Inc.). Final protein concentration was adjusted to 10% total protein of the original, unlabeled serum by diluting with PBS. NSB assays were performed with 10%, 1%, and 0.1% serum (in PBS), corresponding to total protein concentrations of 7.3, 0.73, and 0.073 mg/mL, respectively.

Lysozyme and fibrinogen were assayed in an antibody half-sandwich format. Briefly, assays were performed using standard ELISA-like methods at room temperature with 1 h incubations and PBST rinses. Surface-bound fluorescence signal was measured using a Tecan LS-400 laser scanner.

As a result of fluorescence quenching on ITO and high TCPS autofluorescence during laser scanning, enzyme immunoassays were performed on these surfaces. After incubation (5 μg/mL, 30 min) with the HRP labeled secondary antibody, surfaces were incubated (5 min) with a colorimetric peroxidase substrate (SureBlue, 1-Component TMB, KPL, Inc.) and optical density was read at 450 nm using a plate reader (Dynex Opsys MR).

Control surfaces for both the fluorescence and the enzyme assays were bare and BSA-blocked substrates. BSA blocking was performed by incubating the surface with 5% BSA in PBS for 1 h at room temperature, followed by a PBST then water rinse.

Previous studies have provided reasonable correlation between fluorescence and enzyme-based assays such as those performed here with more quantitative NSB assays.[36,37]

Bacterial Adhesion. Bacterial retention on surfaces was assessed using a custom-built microfluidic device designed to provide well-controlled hydrodynamic conditions.[38] The device comprises plastic laminate assemblies (Aline, Inc.) defining flow channels sandwiched between two transparent coated slides (glass or ITO). Eight independent flow channels, each 10 mm long, 1.7 mm wide, and 0.275 mm deep (rectangular cross section) were observed in real time using darkfield microscopy on an inverted microscope (Olympus IX-70) equipped with a CCD camera (MicroFire). The inlet and outlet ports of each flow channel were fitted with PEEK tubing connected to a custom-built pump station actuating a syringe pump (Kloehn) providing controlled flow delivery in a range from

(32) Gong, P.; Harbers, G. M.; Grainger, D. W. *Anal. Chem.* **2006**, *78*, 2342−2351.

(33) Horbett, T. A.; Weathersby, P. K. *J. Biomed. Mater. Res.* **1981**, *15*, 403−423.

(34) Bergers, J. J.; Vingerhoeds, M. H.; van Bloois, L.; Herron, J. N.; Janssen, L. H.; Fischer, M. J.; Crommelin, D. J. *Biochemistry* **1993**, *32*, 4641−4649.

(35) Unsworth, L. D.; Sheardown, H.; Brash, J. L. *Langmuir* **2005**, *21*, 1036−1041.

(36) Bergstrom, K.; Holmberg, K.; Safranj, A.; Hoffman, A. S.; Edgell, M. J.; Kozlowski, A.; Hovanes, B. A.; Harris, J. M. *J. Biomed. Mater. Res.* **1992**, *26*, 779−790.

(37) Model, M. A.; Healy, K. E. *J. Biomed. Mater. Res.* **2000**, *50*, 90−96.

(38) Busscher, H. J.; van der Mei, H. C. *Clin. Microbiol. Rev.* **2006**, *19*, 127−141.

0.085 to 5 μm/s. These flow rates and channel dimensions result in wall shear rates of 4.6−270 s^{-1}. Two model bacterial strains were used. *Staphylococcus aureus* (ATCC BAA-977) served as model Gram-positive cocci. *Klebsiella pneumoniae* (ATCC 49472) served as model gram-negative rods. These are clinically relevant, pneumonia-causing microorganisms. Fresh (3 h, sub-cultured in tryptic soy broth) cell cultures were centrifuged and re-suspended in PBS at a concentration of 3×10^7 colony forming units (CFU) per mL. Approximately 500 μL of this solution was injected through the flow cell, and then cells settled and were incubated at room temperature with the basal test surface in the absence of flow for 1 h. Images were captured after settling to establish surface baseline cell counts, which were approximately 5×10^4 cells/cm^2. After the static incubation, controlled flow was then initiated and surface images collected for wall shear rates of 4.6, 27, and 270 s^{-1}. Five imaged fields of view were collected for each condition, and custom image analysis software was used to generate adherent bacterial counts. These conditions mimic fluid flow encountered in microfluidic cell culture devices and therefore provide a suitable model.[39]

Safety Consideration. The bacterial strains used here are class II human pathogens. All bacterial assays were performed in a Biosafety Level II Laboratory by trained personnel with proper containment equipment.

Mammalian Cell Adhesion. NIH 3T3 fibroblast (ATCC, MD) adhesion assays were performed on inert polymer-coated surfaces as well as RGD-functionalized polymer surfaces. The first condition was used to demonstrate inhibition of mammalian cell adhesion, while the second demonstrated that the coating can be modified to provide specific functionality, in this case enabling cell attachment via the well-known cell-binding domain, arginine−glycine−aspartic acid (RGD).[40−43]

NHS-activated polymer-coated glass slide pieces (8 × 8 mm) were either (1) immersed in peptide coupling buffer (50 mM sodium borate buffer, pH 7.5, 20.5 h) to hydrolyze the NHS ester to carboxyl groups or (2) incubated in peptide coupling buffer containing the cell-binding peptide, 100 μM GRGDS, for 20.5 h in 24-well plates at ambient temperature (1 sample/well; 500 μL solution/well). TCPS was used as the positive control cell-adhesive surface.

Cell Seeding and Measurement. NIH 3T3 fibroblasts (passage 23; ATCC) were maintained using established methods.[44] Details of the cell seeding and measurement are provided in Supporting Information. Briefly, samples were seeded at 15 000 cells/cm^2 (30 000 cells/well; 24-well Falcon TCPS plate) and incubated (37 °C, 5% CO_2) for 8 and 24 h in growth media (GM) containing 10% serum. At specified times (8 and 24 h), samples were aspirated, rinsed one time with PBS (1 mL) at ambient temperature, replenished with GM, and imaged using an inverted Nikon TE2000-U microscope equipped with a Coolsnap ES CCD camera driven by Metamorph software (Universal Imaging Corp.).

Reproducibility Assays. To assess coating formulation and process reproducibility, three coated glass slide production batches prepared on three different days over a 5 week period were assayed in parallel. Each production batch comprised 300−450 slides, and three slides from each batch were selected to represent the beginning, middle, and end of the coating run. The first assay consisted of an oligonucleotide microarray experiment in which amine-modified and unmodified 40mers were printed onto the amine-reactive coated slides. This assay provided an assessment of NHS activity of the films, with the unmodified oligo serving as an internal NSB control. Details of the oligonucleotide microarray experiment are provided in the Supporting Information. Briefly amine-modified and unmodified 40mer probes with identical sequences were printed to the three slides per batch using a Perkin-Elmer Piezorray noncontact arrayer. After arraying, the slides were incubated for 1 h at 50% humidity and room temperature (∼22 °C) and then deactivated as described in the Surface Deactivation section above. Dye-labeled complementary 40mer target was hybridized for 1 h at 42 °C using Whatman S&S FastFrame chambers. Processed arrays were scanned on a Tecan LS-400 laser scanner. Additional details (buffers, reagent concentrations, times, etc.) are provided in Supporting Information.

As a second assay to test for batch-to-batch variability, the same slides used in the oligo microarray experiment were also checked for protein NSB using 10% fluorescently labeled goat serum as described above. During the oligo hybridization, separate FastFrame chambers were applied to the slides to allow regions to be incubated with the labeled serum. A bare glass slide was used as the positive control in the serum assay.

Results and Discussion

Surface Analysis. *AFM and Ellipsometry*. Representative AFM results are presented in Figure 2. Additional AFM data are provided in the Supporting Information, including topography and phase plots for dry and wet coatings on glass (Figure S1, Supporting Information) and on ITO (Figure S2, Supporting Information). Figure 2a shows that the dry, coated film is very smooth (peak-to-trough roughness of less than 1 nm, rms roughness = 0.29 nm), comparable to the underlying glass substrate. To probe film thickness, the AFM tip was driven into the film and dragged in contact mode to form a scratch (data not shown). Scratch analysis shows a dry film thickness of approximately 20 nm.

Upon hydration, film topography and thickness change significantly, and sequential scans were used to qualitatively monitor film hydration kinetics. Underwater scans (Figure 2b−d) show a small hole defect visible on the right side of the field of view. Line profiles across this defect provide an assessment of thickness and topography evolution: at the 10-min time point, the hole is on the order of 60 nm deep, suggesting that the film has swollen significantly. Subsequent scans over this same location show that the hole largely "heals" over time, presumably from polymer hydration and expansion. Hydrated films reach a stable AFM surface topography after approximately 30 min of water exposure, achieving a final peak-to-trough surface roughness of approximately 10 to 20 nm (rms roughness = 3.20 nm). On the basis of these AFM scratch and hole measurements, dry film thickness on glass is approximately 10−20 nm, while the hydrated film thickness is approximately 50−100 nm with a known peak-to-trough surface roughness of 10−20 nm.

AFM results for polymer-coated ITO surfaces are qualitatively similar to those on the coated glass samples, with the primary difference being the more pronounced film domain structure on ITO (see Figure S2, Supporting Infor-

(39) Li, N.; Tourovskaia, A.; Folch, A. *Crit. Rev. Biomed. Eng.* **2003**, *31*, 423−488.
(40) Drumheller, P. D.; Hubbell, J. A. *Anal. Biochem.* **1994**, *222*, 380−388.
(41) Harbers, G. M.; Healy, K. E. *J. Biomed. Mater. Res., Part A* **2005**, *75*, 855−869.
(42) Hersel, U.; Dahmen, C.; Kessler, H. *Biomaterials* **2003**, *24*, 4385−4415.
(43) Pierschbacher, M. D.; Ruoslahti, E. *Nature* **1984**, *309*, 30−33.
(44) Godek, M. L.; Duchsherer, N. L.; McElwee, Q.; Grainger, D. W. *Biomed. Sci. Instrum.* **2004**, *40*, 7−12.

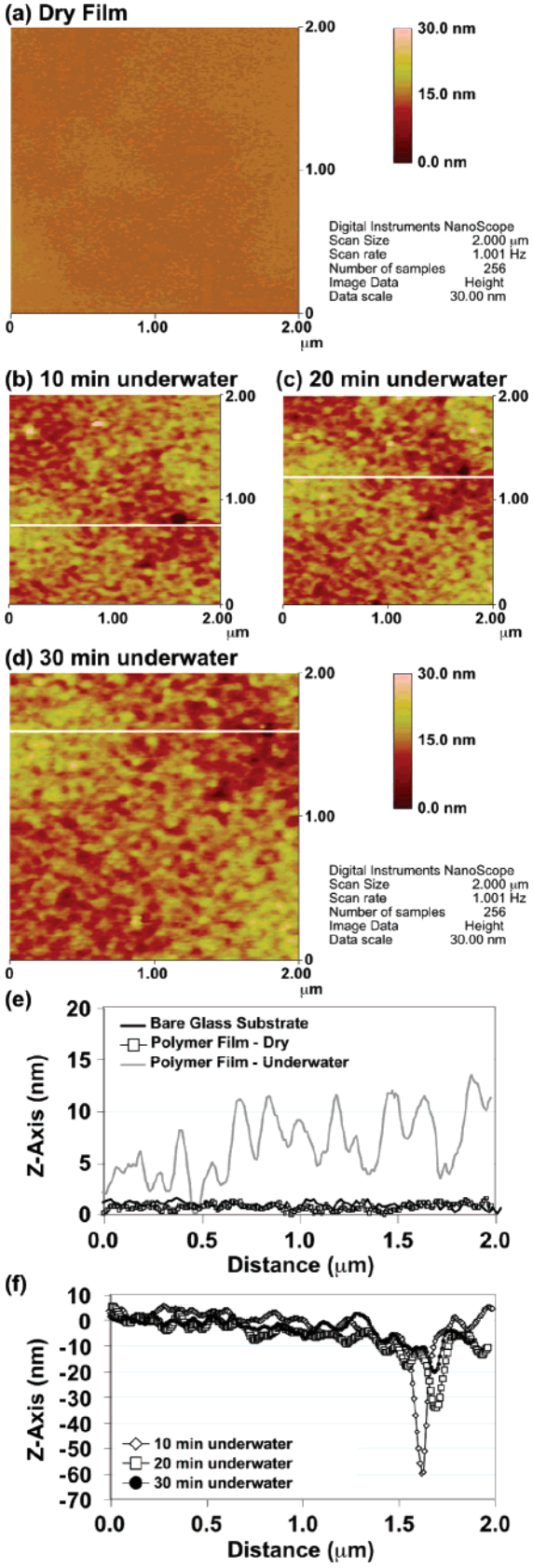

Figure 2. (a) Representative tapping mode AFM topography scan of a dry, polymer-coated glass slide. (b−d) Underwater tapping mode scans after 10, 20, and 30 min of water exposure. (e) Representative AFM line profiles for the bare glass substrate, the dry polymer film, and the hydrated polymer film. (f) Sequence of line profiles showing hydration of the polymer film. These profiles correspond to the lines on images b−d. Note that the image drifts slightly during acquisition of the underwater scans.

mation). It will be shown below that ITO versus glass differences also appear in the XPS data. Despite the physical differences on the two substrates, however, NSB properties of the coating on both substrates are very similar.

AFM results show polymer film thickness and hydration behavior similar to that of PEG films based on adsorbed amphiphiles with intermediate PEG molecular weights (2000−8000)[20] and poly(AAm-*co*-EG) interpenetrating networks.[16] The polymer film is thicker than the more common grafted PEGs, PEG brushes, and SAMs, which have dry film thickness ranging from approximately 1 to 5 nm[10,12,15] depending on molecular weight and coverage.

Spectroscopic ellipsometry data for polymer-coated SiO_2/Si wafers provide dry film thicknesses complementing information generated with AFM. Cauchy model fits were used to estimate polymer thicknesses and optical constants. Polymer thickness was measured at multiple locations on three different wafer substrates, with average dry film thickness of 9.1 ± 0.2 nm. The ∼9 nm thickness result corroborates the AFM conclusion that the cross-linked film is thicker than grafted PEGs and SAMs.

XPS. XPS was used to analyze the NHS-activated polymer-coated glass and ITO surfaces and examine the effects of curing the coating at 100 °C. Table 1 provides compositional XPS data. Additional high-resolution XPS species data are provided in Supporting Information Table S1. XPS-measured surface composition for polymer-coated glass slides shows excellent agreement with the theoretical composition calculated from the input chemical formulation. The carbon/oxygen atomic ratio measured for the polymer film is 2.5, a value consistent with a PEG film enriched with additional carbon, likely from alkyl components of the azidosilane cross-linker and PST matrix-forming molecules. Complete attenuation of glass substrate XPS peaks confirms a relatively thick coating (∼9 to 20 nm based on ellipsometry and AFM). We note here that based on high-resolution Si 2p data (Table S2, Supporting Information), the difference between the theoretical and measured Si 2p signal on glass is not due to substrate detection (i.e., not amorphous silicon oxide), because on glass the Si 2p peak (amorphous Si−O) had a binding energy of 103 eV, while XPS binding energy for the Si 2p peak in the polymer coating was at 102.4 eV, a value more consistent with a silane Si−O peak.

Elemental composition of the polymer film on ITO is similar to that measured on glass. Indium and tin peaks from the substrate, however, are not completely attenuated, suggesting that the coating on ITO is not as thick as that on glass (<5 nm based on XPS sampling depth). This assertion is supported by the C/O ratio of 2.0, suggesting that oxygen from the substrate (ITO) is detected. Presumably, the underlying surface energy or physical features of the ITO affect the polymer coating. The slight differences in the XPS results for ITO versus glass are consistent with the AFM results discussed above.

The combination of AFM, ellipsometry, and XPS provides a reasonably complete picture of film thickness. The dry film is ∼9 nm thick on SiO_2/Si (ellipsometry), approximately 8−20 nm thick on glass (XPS and AFM) and 3−5 nm on ITO (XPS). The varying thickness for the different substrates

Table 1. XPS Elemental Composition Analysis[a] of Polymer-coated and Unmodified Glass and ITO

	element [binding energy[b] (eV)]													
	C 1s (285)	O 1s (532.4)	Si 2p (103)	N ls (401.8)	Cl 2p (199.7)	S 2p	Al 2p (74.2)	K 2p (293.6)	Na 1s (1072.2)	Ti 2p (459.5)	Zn 2p3 (1022.7)	B 1s (192.8)	In 3d5 (443.9)	Sn 3d5 (485.8)
bare glass	9 (0.7)	61.8 (0.4)	22.1 (0.6)	1 (0.0)	0.1 (0.0)	nd nd	1.9 (0.1)	0.7 (0.1)	0.5 (0.1)	0.6 (0.0)	0.5 (0.1)	1.8 (0.1)	nd	nd
polymer-coated glass	67.6 (1.6)	27.3 (2.0)	2.1 (0.1)	1.8 (0.2)	0.3 (0.1)	0.9 (0.3)	nd	nd	nd	nd	nd	nd	nd	nd
bare ITO	13.5 (1.3)	52.7 (1.3)											30.1 (0.2)	3.7 (0.2)
polymer-coated ITO	64.3 (0.8)	31.5 (0.6)	1.3 (0.1)	0.9 (0.1)	<0.1	0.3 (0.1)	nd	nd	nd	nd	nd	nd	1.4 (0.3)	0.3 (0.1)
polymer coating (theoretical)	69.7	27.2	0.5	2.1		0.4								

[a] All values are atomic percents, with standard deviation in parentheses. [b] Binding energies are provided for reference and are only approximate.

is not unexpected, given that spin-coated film thickness depends in part on the surface energy of the substrate. Upon hydration, the films expand significantly to thicknesses of 50−100 nm.

Cure Analysis. High-resolution XPS and Fourier transform infrared (FTIR) spectra were used to gain insight into the chemical evolution of the azidosilane cross-linker. Detailed XPS and FTIR results and discussion are provided in the Polymer Cure Study section of the Supporting Information. Results presented there are consistent with a fractional conversion of the azide to nitrene with subsequent insertion into aliphatic carbon chains in the coating, suggesting the desired cross-linking reactions indeed occur.

Contact Angle. Clean, uncoated glass and ITO substrates exhibited water contact angles of less than 10°. Uncoated TCPS dishes had contact angles of approximately 57°, consistent with literature values.[45] Static contact angles of the NHS-activated coatings were 62.0 ± 1.5° for glass, 54.4 ± 2.1° for ITO, and 60.7° ± 0.6° for TCPS. Deactivation with MEA results in contact angles of 49.6 ± 3.4° for glass, 46.7 ± 3.3° for ITO, and 59.2 ± 0.7° for TCPS. Average intra-slide (six-spot) coefficients of variation were less than 6% for all substrate types.

These coatings are less hydrophilic than the most common PEG-based hydrogel chemistries, which typically show water contact angles between 30° and 40°.[15,16,25,46−48] The decrease upon deactivation is the result of removing the NHS leaving group and replacing it with a mixture of terminal methoxy and carboxyl groups (the latter due to competing hydrolysis reactions). The slightly lower contact angles for coated ITO correlate with the AFM results (Figure S2, Supporting Information) showing an altered surface microstructure on this substrate.

Dynamic water contact angles measured on polymer-coated glass slides ($n = 6$) showed advancing (68.7 ± 0.7°) and receding (14.8 ± 2.0°) angles with a hysteresis of 53.9°. This is a large but not unprecedented hysteresis. Observed hysteresis is attributed to large PEG tethered chain mobilities[49] that respond to the moving three-phase line and is not ascribed to surface topological effects. An alternative explanation for large hysteresis would be release of surface-active components from the film into the test droplet during the measurement (e.g., leaching). This was ruled out by comparing droplet surface tension before and after exposure to the polymer surface. Large hysteresis is not uncommon for swellable hydrogels,[50,51] but this behavior is different from SAMs or grafted PEG brushes where the hysteresis is smaller, typically on the order of 9−15°.[15,25,48]

Protein NSB. Protein NSB results for fluorescent assays on coated glass slides are presented in Figure 3. Results show that the polymer film provides significant inhibition of serum-based NSB. For 10% serum, the polymer provides 97% reduction in nonspecifically adsorbed serum components, with even better percent reductions in more dilute serum. This result suggests that the polymer coating is particularly good at inhibiting adsorption of the primary albumin and globulin protein components that comprise the largest protein fractions (>90%) in serum. The coating provides a 90% reduction in fibrinogen NSB relative to bare glass control at 100 μg/mL fibrinogen, although the relative reduction was not as good for 10 μg/mL fibrinogen (73% reduction). Lysozyme NSB was also significantly inhibited. At 100 μg/mL lysozyme, the coating provided greater than 95% reduction in NSB relative to bare glass. For all three protein systems (serum, fibrinogen, lysozyme), the polymer-coated glass slides out-performed BSA-blocked glass slides.

Figure 3d,e shows fibrinogen NSB on ITO- and TCPS-coated surfaces measured by enzyme immunoassay. Reduction of fibrinogen NSB was similar to that seen on coated glass. Performance of the polymer-coated ITO and TCPS surfaces was comparable to BSA-blocking, suggesting that BSA-blocking works better on ITO and TCPS than it does on glass, an expected result given that BSA blocking is best on surfaces that present hydrophobic surface sites.[1] Note also that the 0 μg/mL fibrinogen control wells yield relatively strong NSB signals on the bare ITO and TCPS surfaces, a

(45) Koenig, A. L.; Gambillara, V.; Grainger, D. W. *J. Biomed. Mater. Res.* **2003**, *64*, 20−37.
(46) Harbers, G. M.; Gamble, L. J.; Irwin, E. F.; Castner, D. G.; Healy, K. E. *Langmuir* **2005**, *21*, 8374−8384.
(47) Herrwerth, S.; Eck, W.; Reinhardt, S.; Grunze, M. *J. Am. Chem. Soc.* **2003**, *125*, 9359−9366.
(48) Pale-Grosdemange, C.; Simon, E. S.; Prime, K. L.; Whitesides, G. M. *J. Am. Chem. Soc.* **1991**, *113*, 12−20.
(49) Karlsson, J. O.; Gatenholm, P. *Macromolecules* **1999**, *32*, 7594−7598.
(50) Andrade, J. D., Ed. *Surface and Interfacial Aspects of Biomedical Polymers*; Plenum Press: New York, 1985.
(51) Emoto, K.; Nagasaki, Y.; Kataoka, K. *Langmuir* **1999**, *15*, 5212−5218.

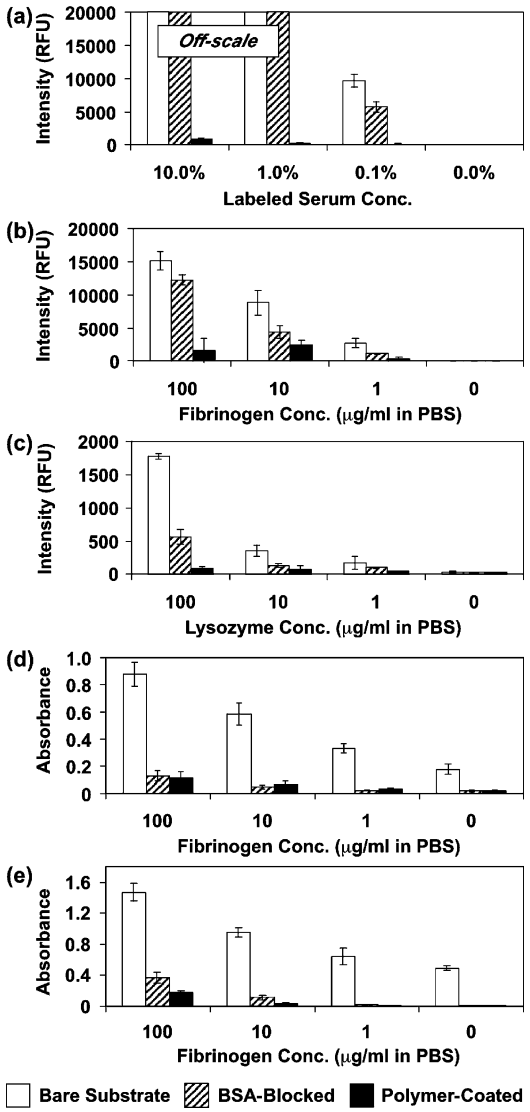

Figure 3. (a−c) Fluorescently labeled protein NSB on uncoated, BSA-blocked, and polymer-coated glass slides. (a) Dye-labeled serum NSB. The bars are off-scale for the bare and BSA-blocked glass at 10% and 1% serum. Fluorescence intensity values for bare glass are 32 293 and 28 776 RFU (10% and 1% serum, respectively) and are 39 132 and 29 103 RFU for BSA-blocked glass. (b) Human fibrinogen and (c) lysozyme NSB on glass slides using the fluorescent half-sandwich assays. For parts a−c, RFU = relative fluorescence units as generated by the Tecan laser scanner on the green (532 nm) channel at 55% PMT; values reported for each concentration are three slide averages, with error bars representing one interslide standard deviation. (d) Human fibrinogen NSB to ITO and (e) TCPS as measured by enzyme immunoassay. Absorbance units are optical density at 450 nm. Values reported for each concentration are three slide averages and three wells per slide (nine wells total), with error bars representing one standard deviation.

result of NSB of anti-fibrinogen antibody to these surfaces. The polymer coating completely inhibits this effect without the use of special blocking reagents in the diluent buffer.

Inhibition of Bacterial Adhesion. Bacterial retention assay results are presented in Figure 4. *S. aureus* adhesion to bare glass and bare ITO surfaces is strong and largely irreversible after 1 h of static incubation in the flow cell. Even at a wall shear rate of 270 s^{-1} (data not shown), >60% of the *S. aureus* microorganisms remained bound to the glass surface, and >80% remain bound to bare ITO. In contrast, essentially all *S. aureus* cells were removed from polymer-coated surfaces at the lowest shear rate, suggesting that adhesion to the polymer surface is weak in the time frame tested.

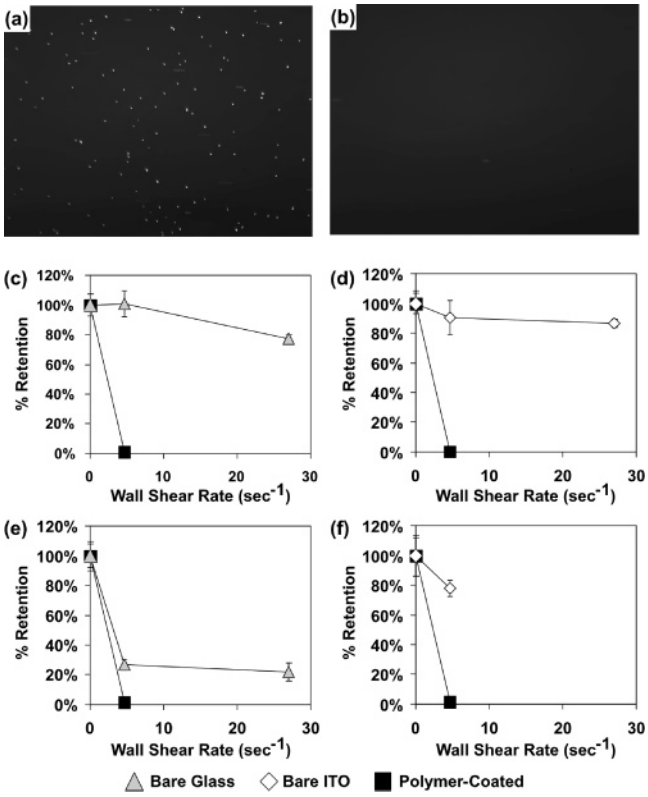

Figure 4. Bacterial adhesion to bare and polymer-coated surfaces in a microfluidic flow cell. (a) Representative image of a bare glass flow cell surface after *S. aureus* exposure and rinse at a shear rate of 4.6 s^{-1}. (b) Image of polymer-coated surface under same conditions as in part a. Streaks in the images are bacteria moving laterally during the image exposure (not counted in the analysis). (c) Percent retention of *S. aureus* on bare and polymer-coated glass flow cell surfaces at different rinse wall shear rates. (d) *S. aureus* retention on ITO. (e) *K. pneumoniae* retention on glass. (f) *K. pneumoniae* on ITO. Values are normalized cell counts averaged over five microscope fields of view. Error bars represent one standard deviation.

Results for *K. pneumoniae* were similar. *K. pneumoniae* is less adherent to bare glass than *S. aureus*, consistent with the fact that different bacterial strains and species exhibit widely different adhesive properties.[38] *K. pnuemoniae* cells were completely removed from the polymer coated surfaces at the lowest shear rate (4.6 s^{-1}). For these representative strains, performance is qualitatively comparable to that seen on ethylene oxide-terminated SAMs[27] and long chain-length PEG brushes.[52] It is important to reiterate that these data are for short-term bacterial exposure (1−2 h). This time frame was selected because it is particularly relevant to in vitro bioassays. Additional bacterial adhesion studies, including 7 day coating stability assessment in biological fluids, are published elsewhere.[53]

Mammalian Cell Adhesion. Figure 5 presents NIH 3T3 fibroblast 24-h adhesion data from 10% serum-containing media to the inert (i.e., hydrolyzed) polymer coating, GRGDS-modified-polymer coating, and the TCPS positive control. Figure 5a shows virtually no fibroblast adhesion to the hydrolyzed polymer-coated surface in the 24-hour culture test, a result consistent with the inhibition of protein and

(52) Roosjen, A.; Boks, N. P.; Van der Mei, H. C.; Busscher, H. J.; Norde, W. *Colloids Surf., B* **2005**, *46*, 1−6.
(53) Saldiagarra Fernandez, I. C.; van der Mei, H. C.; Lochhead, M. J.; Grainger, D. W.; Busscher, H. J. *Biomaterials* **2007**, *28*, 4105−4112 (http://dx.doi.org/10.1016/j.biomaterials.2007.05.023).

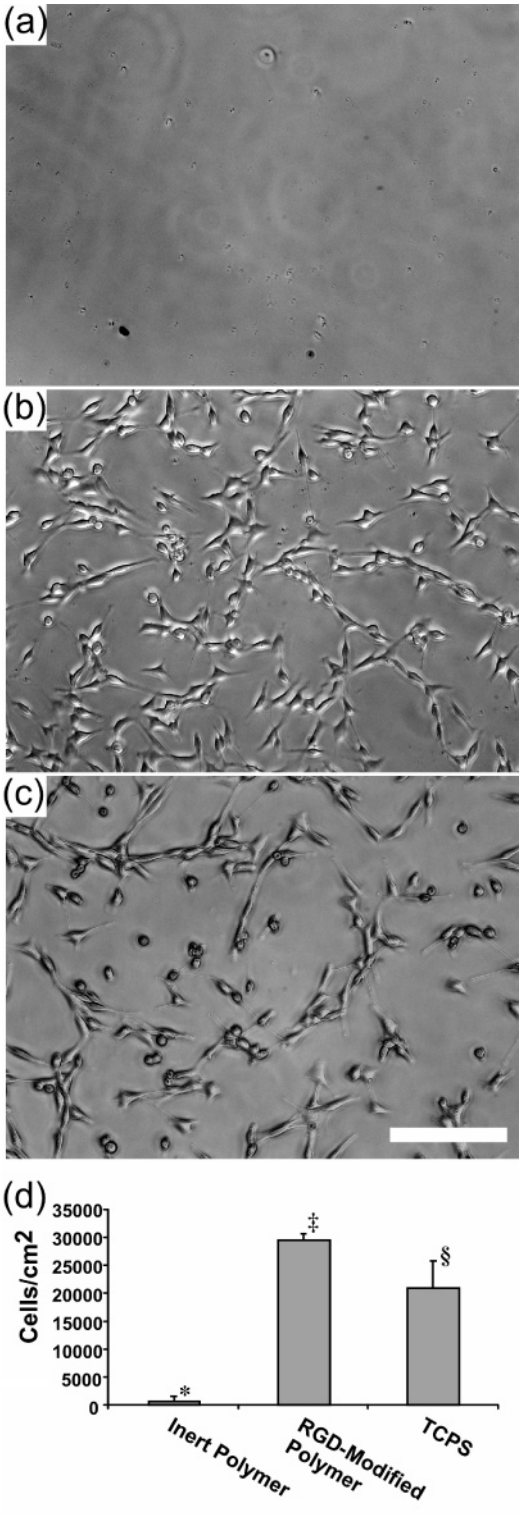

Figure 5. NIH 3T3 fibroblast adhesion (24 h) to the inert polymer surface, GRGDS-modified polymer surface, and TCPS in 10% serum-containing media. Representative images for each surface: (a) hydrolyzed "inert" polymer coating; (b) GRGDS-modified polymer; and (c) TCPS positive control. (d) Total cell number determined using digital image analysis; surfaces not in the same group (*, §, ‡) were statistically different from one another ($p < 0.05$; ANOVA with Tukey Kramer post-hoc test). Scale bar = 200 μm.

bacterial adhesion presented already. The RGD-functionalized coating, however, showed significant NIH 3T3 cell attachment, including greater attachment than even the TCPS control (Figure 5b,c). Figure 5d provides a quantitative analysis of cell attachment for the three surfaces. This last

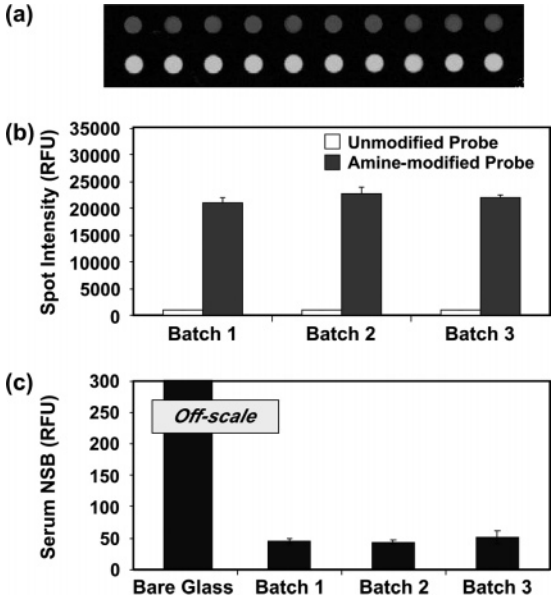

Figure 6. Batch-to-batch reproducibility data. (a) Representative microarray image of unmodified (top row) and amine-modified (bottom row) oligos printed onto the polymer coating and then hybridized with dye-labeled oligo target. (b) Oligo microarray assay results and (c) dye labeled serum NSB results for three representative production batches prepared over a 1 month period. Three slides per batch were assayed; each bar represents a three slide mean and the error bars represent ± one standard deviation. Signal for the bare glass control in the serum assay is off-scale at 18 701 RFU (RFU = relative fluorescence units).

plot shows that the nonfouling surface chemistry is readily functionalized to actively promote specific adhesion.

Reproducibility Assays. Figure 6a,b presents results for the oligonucleotide microarray assay. Reproducibility is reported as percent coefficient of variance (%CV), defined as %CV = 100 × (standard deviation/mean). Intra-batch reproducibilities of amine reactivity as measured by the amine-modified oligo spot signal (10 spot subarrays, two subarrays per slide, three slides per batch; 60 spot statistics) were 5.4%, 5.2%, and 2.0% CV for the three batches tested. Inter-batch reproducibility was 4.1% CV for the three batches assayed here. Specificity of the NHS to amine-oligo is demonstrated by the very low signal seen on the unmodified-oligo probe spots.

The serum assay data show quantitative results very similar to those presented in Figure 3, with the coated slides giving < 1% of the NSB signal seen on the bare glass controls. Reproducibility of the serum NSB signal for the three batches tested was 7.2% CV.

Regarding reproducibility, we also note here that this formulation has been used in over 400 quality controlled production batches constituting more than 45 000 coated substrates distributed worldwide for microarray applications.

Conclusions

A novel, multicomponent, cross-linked polymer surface chemistry that effectively inhibits the nonspecific adsorption of proteins, bacteria, and mammalian cells has been described and characterized. The coating is unique in the context of PEG surface chemistries in that it comprises a simple, commercially viable, single-step coating process applicable to a variety of solid substrate materials. Further, the polymer

surface chemistry can be modified in situ to provide specific attachment chemistries within the same low NSB coating matrix. The coating technology is particularly relevant for in vitro bioassay applications where the combination of low NSB and highly specific immobilization is required for assay sensitivity. The long-term stability of this coating in biological milieu is the subject of parallel studies.[53]

Acknowledgment. Partial support from NIH Grant EB1473 (to G.M.H. and D.W.G.) is acknowledged. We thank Dr. G. Mao for technical advice regarding the coating formulation chemistry, Y.-F. Lu and Dr. B. Parkinson, Colorado State University (CSU), for assistance with AFM measurements, Dr. E. Fisher (CSU) for use of the dynamic contact angle tool, and Dr. S. Kohli and D. Heyse (CSU CIF) for assistance with ellipsometry measurements.

Supporting Information Available: Additional experimental details and AFM, XPS, and FTIR data (PDF). This material is available available free of charge via the Internet at http://pubs.acs.org.

CM070509U